Implementation of a DSP-based hybrid sensor for switched reluctance motor converter

Whei-Min Lin[1], Chih-Ming Hong[1], Chiung-Hsing Chen[2], Huang-Chen Chien[1]

[1]Department of Electrical Engineering National Sun Yat-Sen University, Kaohsiung 80424, Taiwan, R.O.C.
[2]Electronic Communication Engineering, National Kaohsiung Marine University, Kaohsiung 81157, Taiwan, R.O.C

Abstract
The Switched Reluctance Motor (SRM) inherits a simple and reliable structure with an economical manufacturing cost. The DC power output supplies the unipolar converter to control the pulses sent to SRM. Thus, the velocity and torque are controllable for various velocity commands, and the SRM is gaining more and more applications on high torque requirement field with constant power. This paper proposes a DSP based hybrid sensor for switched reluctance motor with easy implementation. The current transducer is used to monitor the energized current and proximity sensors for rotor salient. The signals are then fed back to DSP. This design will improve the performance of SRM to operate more smoothly.
Copyright © 2010 International Energy and Environment Foundation - All rights reserved.

Keywords: Switched reluctance motor, Current transducer, Proximity sensor.

1. Introduction
The recent surge of interest in switched reluctance motor (SRM) has started due to the demand for variable speed drives in consumer and industrial products, such as washing machine, fans, motorbike and automobile. To save energy and our planet, the fossil-fuel engine pollution causes greenhouse gases to warm the atmosphere. The emerging motor driver applications for variable speed drives need to be extensively developed. Why SRM? Demanding higher reliability and an equivalent performance to the dc and induction motor drives are very cost sensitive. The SRM drive system is very promising to meet such demands in a cost effective fashion, hence the activities in this field will grow up.
SRM is designed for efficient power conversion for high speed applications. It inherits low manufacturing cost and rugged structure, and the SRM has been considered to be brushless at a low cost with equivalent performance to compare with AC motor drives. The earliest recorded SRM was the one built by Davidson in Scotland in 1838 and was used to propel a locomotive on the Glasgow-Edinburgh railway near Falkirk [1]. Since mid-1960s, these developments have given SRM a fresh start and raised its performance to level competitive with AC, DC and brushless DC drives [2].
SRM has a significant torque ripple because of the double salient structure. There were many researches proposed on issues of the modified salient pole shape profile and the specific design for motor phase number, flux path and air gap parameters to achieve the efficiency and smoothness improvement [1-3]. In general, the converter efficiency is tradeoff between the controller improvement and driver cost. A

simple and robust controller for ease practical applications is the most challenge task [3].

The SRM geometry of rotor and stator has non-linear and time-varying characteristics. Several optimizing efficiency strategy is proposed to estimate the parameter and linearity the SRM model [3]. To reduce the rotor sensor cost, the sensorless algorithm was proposed as observer of flux-linkage and phase current. And also, the modulation frequency technique was considered [4, 5]. This paper proposed a digital signal processor (DSP) based hybrid sensor for switched reluctance motor. The algorithm is easy to be implemented. It uses the current transducer to monitor energized current and the proximity sensors apply to sense the rotor salient. They cooperate to feed back the signal to the DSP. This feature will improve the SRM at various speeds with smoothly spin performance.

2. Dynamic model of a SRM

SRM dynamic model's equations are derivative in this section. These equations govern the velocity estimation and torque output in the closed-loop control algorithm.

2.1 Equivalent circuit of a SRM

A single phase equivalent circuit is shown in Figure 1, where suffix x means phase a, b, and c and assume the same phase winding of stator to be serial into a resistance and inductance.
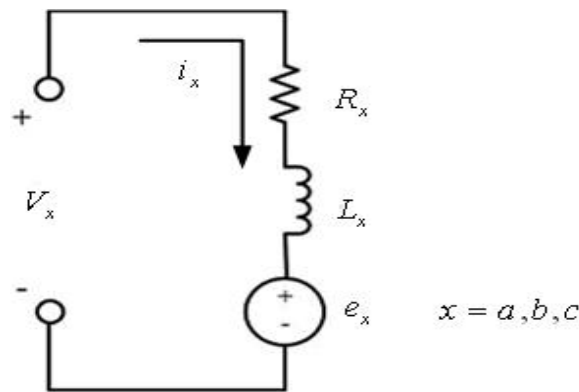

Figure 1. Single phase equivalent circuit

The phase voltage equation of SRM can be expressed in the form of

$$V_a = i_a \cdot R_a + \frac{d\lambda_a}{dt} \tag{1}$$

$$V_b = i_b \cdot R_b + \frac{d\lambda_b}{dt} \tag{2}$$

$$V_c = i_c \cdot R_c + \frac{d\lambda_c}{dt} \tag{3}$$

where λ_a、λ_b、λ_c are flux linkage of phase a, b and c, respectively

$$\lambda_a = i_a \cdot L_{aa} + i_b \cdot L_{ba} + i_c \cdot L_{ca} \tag{4}$$
$$\lambda_b = i_a \cdot L_{ab} + i_b \cdot L_{bb} + i_c \cdot L_{cb} \tag{5}$$
$$\lambda_c = i_a \cdot L_{ac} + i_b \cdot L_{bc} + i_c \cdot L_{cc} \tag{6}$$

where: V_a、V_b、V_c are stator winding phase voltage, R_a、R_b、R_c are stator winding resistance, i_a、i_b、i_c are stator winding phase current, L_{xy} $x, y = a,b,c$: $x = y$ self-inductance of the phase $x \neq y$ mutual-inductance of the phase

2.2 Torque equation

The torque is produced in the SRM by the radial and tangential flux density components interaction. The electromagnetic torque of the SRM is a nonlinear function of the stator current and rotor position θ.

The equations illustrate above will be utilized to establish the SRM output torque estimation model; the assumption nonlinearly magnetic operation and certainly the nonlinear effect are taken into account.

Multiplying (1) to (3) by the current result in input power, given by

$$V_x \cdot i_x = i_x{}^2 \cdot R_x + i_x \cdot \frac{d\lambda_x}{dt} \tag{7}$$

where: $V_x \cdot i_x$: input power, $i_x{}^2 \cdot R_x$: winding resistive losses (Ohmic losses), $i_x \cdot \frac{d\lambda_x}{dt}$: filed energy

The last term of equation (7) is filed energy to be express as

$$i_x \cdot \frac{d\lambda_x}{dt} = \frac{dW_m}{dt} + \frac{dW_f}{dt} \tag{8}$$

where: $\frac{dW_m}{dt}$ is instantaneous mechanical power, $\frac{dW_f}{dt}$ is instantaneous magnetic field power.

Mechanical power equation can be expressed in a more conventional way multiplying torque with rotor speed, as follows:

$$\frac{dW_m}{dt} = T_e \cdot \omega_m = T_e \cdot \frac{d\theta}{dt} \tag{9}$$

where: T_e is electromagnetic torque, ω_m is rotor speed.

Substituting (9) into (8) gives

$$i_x \cdot \frac{d\lambda_x}{dt} = T_e \cdot \frac{d\theta}{dt} + \frac{dW_f}{dt} \tag{10}$$

The torque is obtain by the equation

$$T_e(\theta, \lambda_x) = i_x(\theta, \lambda_x) \frac{d\lambda_x}{d\theta} - \frac{dW_f(\theta, \lambda_x)}{d\theta} \tag{11}$$

Assuming constant flux gives general expression of the torque by one phase,

$$T_e = -\frac{dW_f}{d\theta} \tag{12}$$

where W_f is stored field energy,

$$W_f = \int_0^{\lambda_x} i_x(\theta, \lambda) d\lambda_x \tag{13}$$

At any position, the co-energy is the area below the magnetization curve as in Figure 2. In here, co-energy and stored filed energy chart is shown.

Definite integral as

$$W_c = \int_0^{i_x} \lambda_x(\theta, i) \, di_x \tag{14}$$

where W_c is co-energy at constant current and the rotor moving through an infinitesimal displacement. The energy conversion is illustrated by the co-energy trajectory. The W_c area represents the energy converted into mechanical energy. W_f returns the energy to the power supply rails.
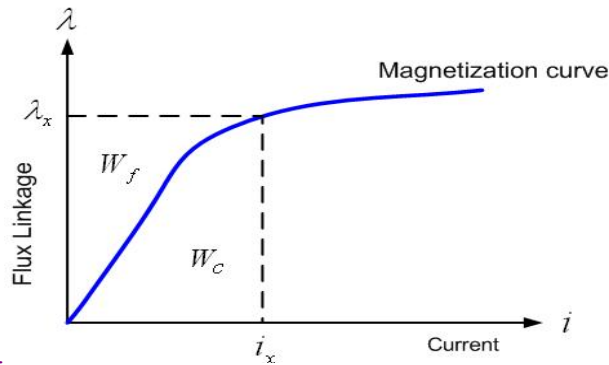

Figure 2. Co-energy W_c and stored field energy W_f

The co-energy and stored field energy are given by

$$W_c + W_f = i_x \cdot \lambda_x \tag{15}$$

Differential result as

$$dW_c + dW_f = \lambda_x \cdot di_x + i_x \cdot d\lambda_x \tag{16}$$

Substituting dW_f of the equation (16) into (11), delivers:

$$T_e = \frac{i_x d\lambda_x - [\lambda_x di_x + i_x d\lambda_x - dW_c(\theta, i_x)]}{d\theta} \tag{17}$$

As the current increases, the torque increases, too. At low current scope, the torque is roughly proportional to the current squared. At higher currents, it becomes nearly linear. At very high current scope, the flux saturation decreases the torque per ampere. Figure 3 show general torque / speed characteristic of a SRM.
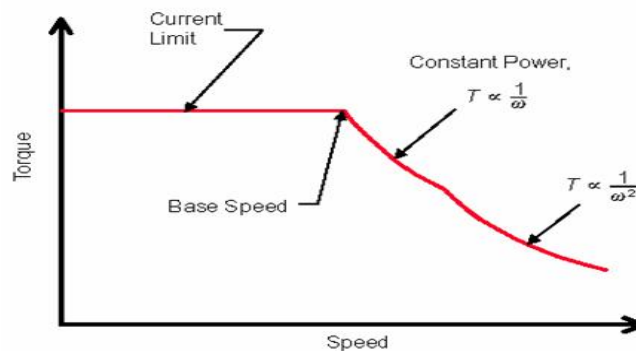

Figure 3. General torque / speed characteristic of a SRM

3. Implementation of DSP-based SRM drive system

A Texas Instruments (TI) TMS320F240 DSP is used as the controller to drive the SRM system. The prototype system is formed by five subsystems. These subsystems are power MOSFET gate driver, inverter, closed-loop current transducer circuit, closed-loop proximity circuit and command interface circuit. The DSP -based SRM drive system scheme is shown in Figure 4.

3.1 Closed - loop current transducer circuit

Current transducer is a non-contact to measure the current device. The transducer is winding over the wire carrying the current to be measured, and the transducer secondary wires are connected with the voltage coupler to obtain the voltage, and feedback to DSP ADC converter. Figure 5 is shown the closed-loop current transducer circuit.

This paper uses three sets of current transducer for three phase current measurement. The feedback to ADC converter can be obtained as

$$V_{out} = i_{phase} \cdot N_1 \cdot K_N \cdot VR \tag{18}$$

where: V_{out} is closed-loop current transducer output voltage, N_1 is the winding numbers on current transducer, K_N is conversion ratio, i_{phase} is phase winding current, VR is measuring resistance.
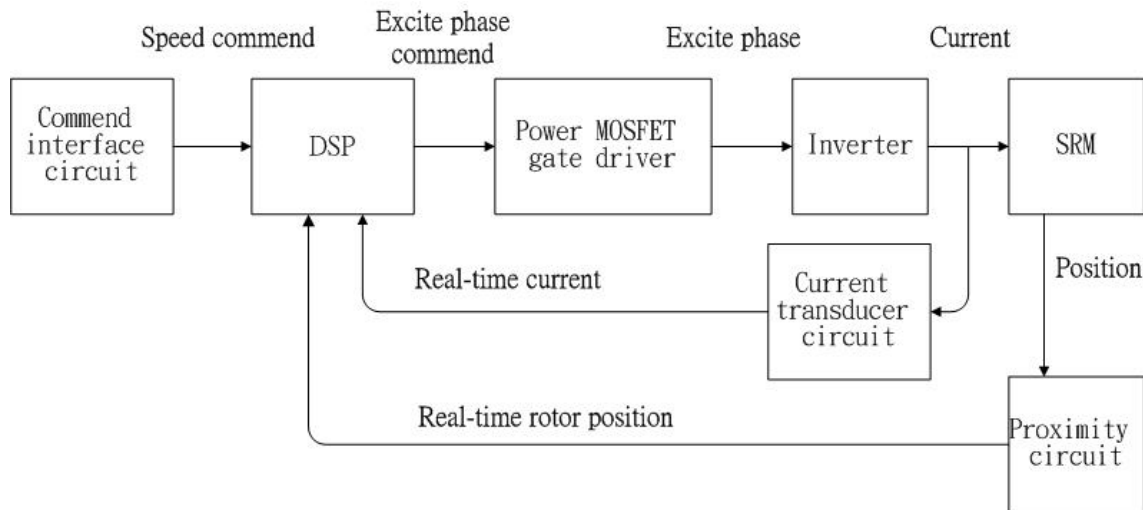

Figure 4. The system configuration of a SRM drive system
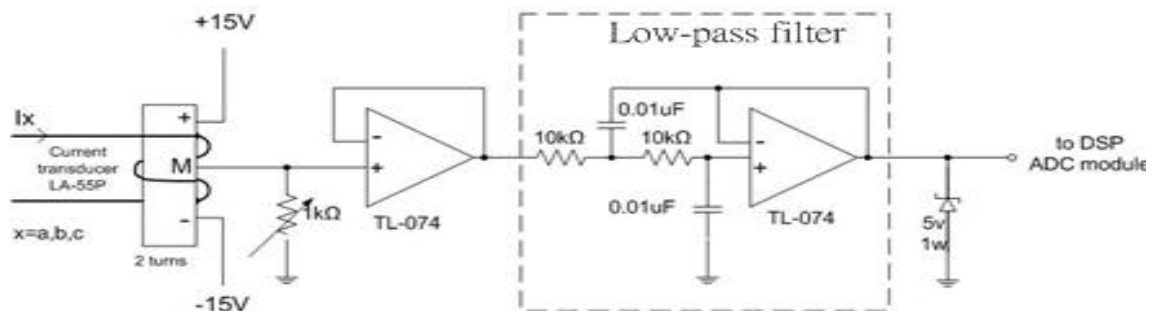

Figure 5. Closed-loop current transducer circuit

3.2 Closed - loop proximity sensor circuit

The sensing device generates one pulse per pass of an actuating target within its sensing field. No direct contact with the target material is necessary. Each sensor is entirely solid state with no moving parts to wear out. This provides for long life with little or no maintenance requirement [6-10].

In this paper, three sets of capacitive proximity sensors are used for SRM operation with rotor position to

feedback to the DSP for communication. The sensors location is illustrated with Figure 6. The rotor salient of the present is to provide proximity sensors employing impulse waves. For low cost SRM drives, proximate position sensors have been use to sense rotor salient directly.

Base on the proximate sensors feedback, DSP assigns which phase winding should be energized in an optimal control to achieve smoothly, continuous torque and high efficiency rotation. Furthermore, the position angle between two proximity sensors signals is estimated in the software program.

(a)   (b)
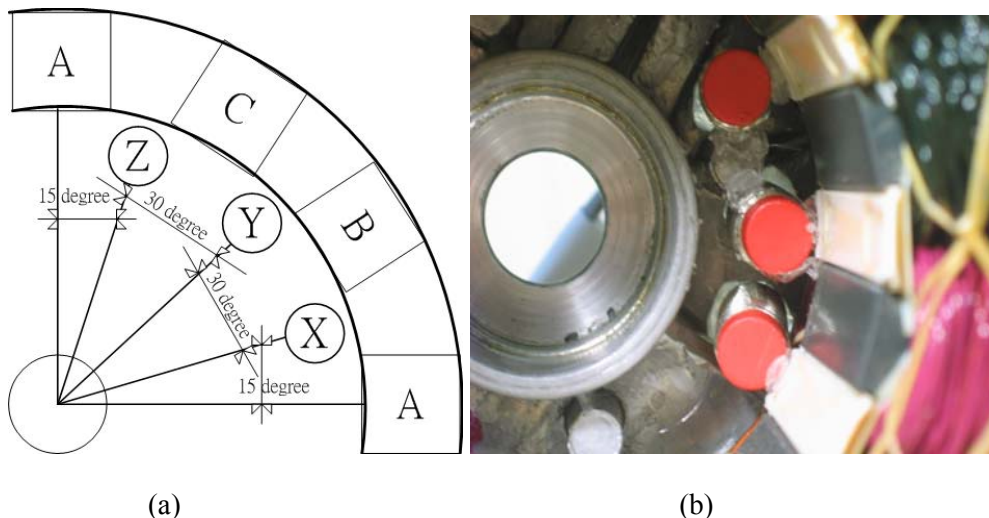
Figure 6. (a) proximity sensor in the stator configuration, and (b) accomplish picture

The Table 1 illustrates the truth value of energizing to the stator winding of phase A, B, C when S_x, S_y, S_z proximity sensor status results rotate direction. The stator winding is energized every 15 rotor mechanical degrees, and the transition state during the 15-degree angle is also shown for clarification. Figure 7 illustrates the relationship between the energizing stator winding pole A and rotor salient position. The proceeding of salient pole 1 through stator A winding can be seen in this Figure. An increasing stator current results in enhancing SRM mechanical power output, but the enhancement of mechanical energy is not uniform for all of the operating. Particularly in the saturated region, it should be avoided the align area operation.

Table 1. The truth table of A、 B、 C proximity sensor status

Rotor mechanical degree	S_x	S_y	S_z	Energized phase (Clockwise)	Energized phase (Counterclockwise)
0~7.5	0	1	0	B	C
7.5~15	1	1	0	A	B
15~22.5	1	0	0	A	B
22.5~30	1	0	1	C	A
30~37.5	0	0	1	C	A
37.5~45	0	1	1	B	C

3.3 Command interface circuit

For convenient operation, the command interface is accessible for full range of commands. It is an implement for switching the SRM to assign rotation direction and obtain velocity command. The circuit is shown in Figure 8, it consists of a variable resistor (VR), voltage follower and two switches.

One of the switches is enabling the SRM controller; the other assigns rotate direction command. The VR and voltage follower regulate analog DC voltage from 0 to 5 volt. This signal is converted by the DSP ADC converter to a digital value between 0 to 1023; this corresponds to a SRM velocity command from 0 to 3000 rpm. Each digit has a step of around 3 rpm. Especially for user interested in changing the speed during operation, the command interface is very useful to input new velocity commands to the DSP.
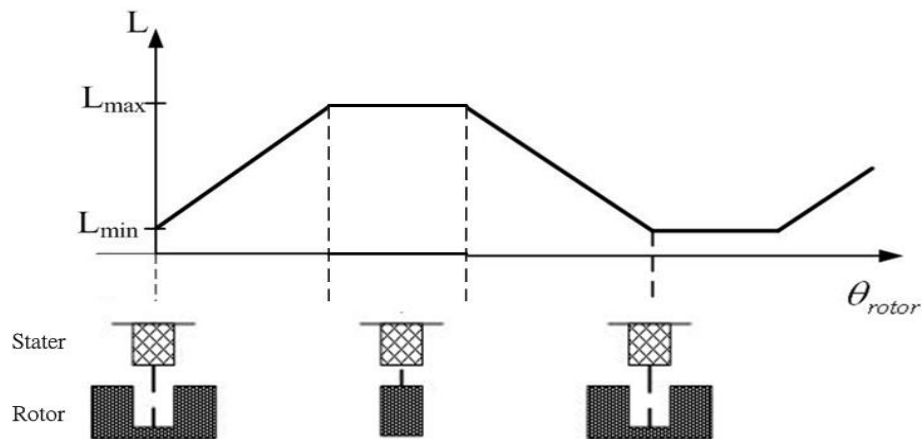
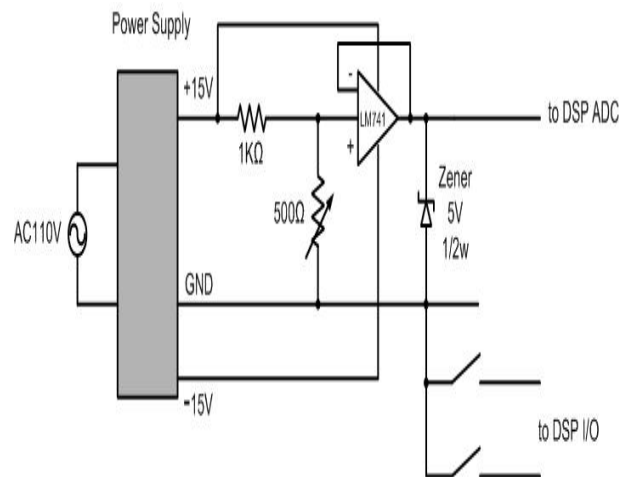Figure 7. Idealized inductance profile vs. rotor salient position

Figure 8. Command interface circuit

4. Design of control system

The operation of SRM winding is activated only one phase at a cycle time. DSP is required in the presence of current constraint with closed-loop PWM. The overall DSP based control system is illustrated in Figure 9.
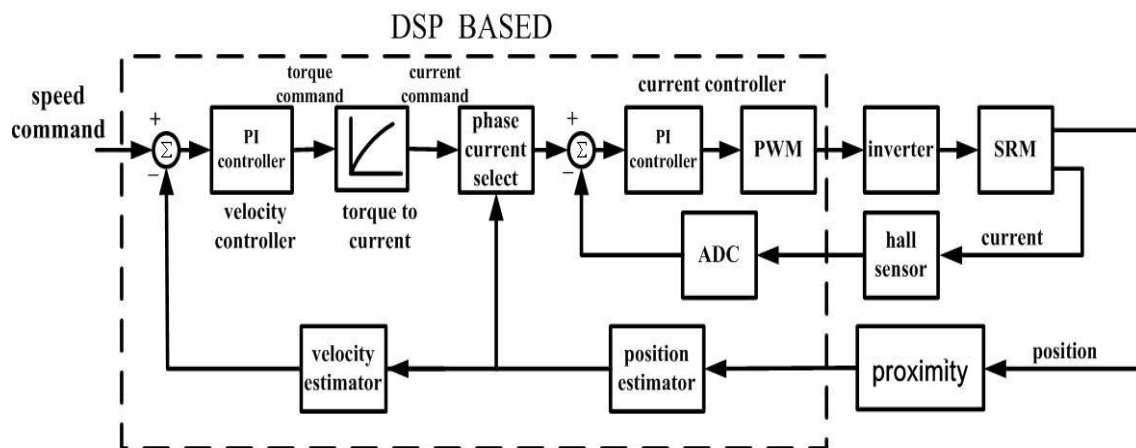

Figure 9. The SRM control system block diagram

4.1 Software structure
4.1.1 Main program
The main program initializes for the counters, flags, interrupts and the event manager. The event manager initialization respectively configures the timer units, ADC converter, input/output ports and the PWM Compare Units in the continuous counting mode. It generates the fixed-frequency carrier PWM to compare with velocity command to control phase current. The subprogram consists of several algorithms for the SRM control and operation, they are elaborated in following Figure 10.
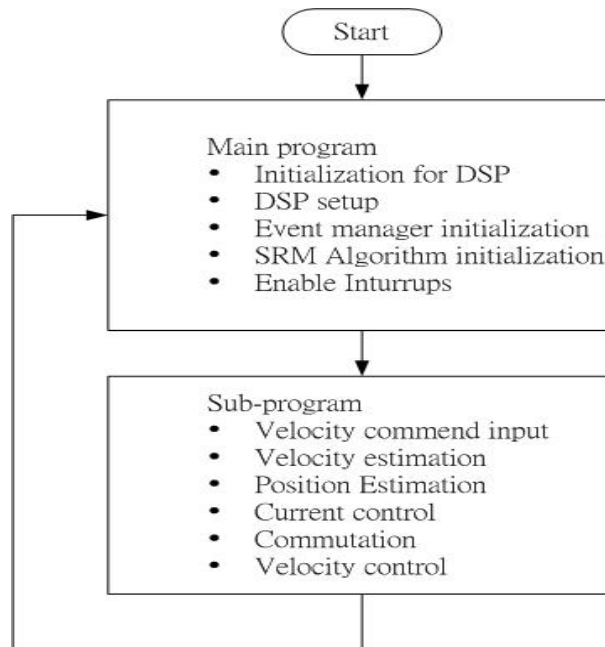
Figure 10. Overview of the SRM control program

4.1.2 Hybrid sensors communication and phase current algorithm
Three proximate sensors infer the rotor salient position to decide which phase should be energized; the truth table is shown in Table I. For motoring operation, the pulses of phase current must coincide with a period of increasing inductance. Figure11 represents the effect of energizing phase winding while a pair of rotor poles is approaching to align with the stator poles. If it separates from alignment position at next cycle, the proximity sensors change status and feedback to the ADC converter at the same time.
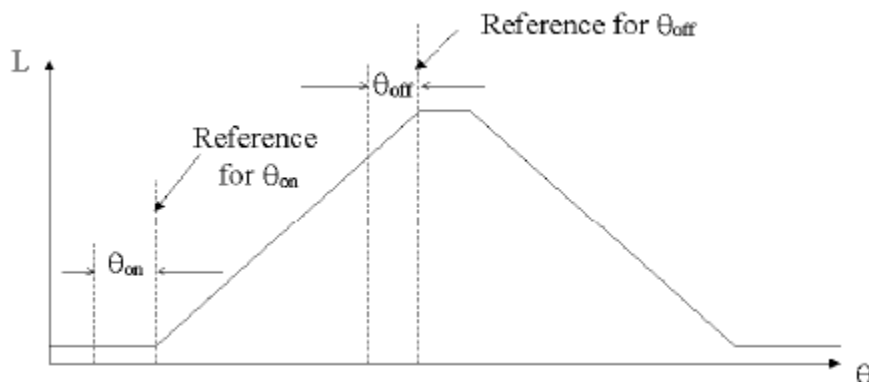

Figure 11. Turn-on and turn-off angles of SRM

The switching feature is to ensure that the phase winding current reaches its reference value at the desired instantaneous of inductance rise, then brought again to zero when inductance reaches its maximum. Due to the delay in current rise and fall on account of winding inductance, the switching must be opened at a turn-on angle and must similarly be closed at a turn-off angle as in Figure 12.
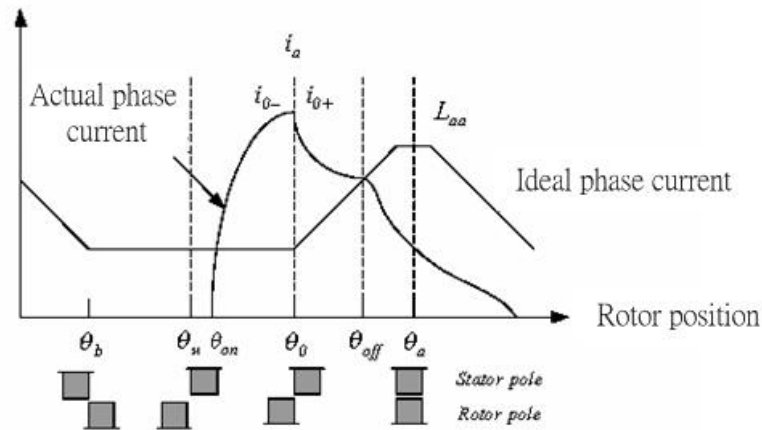
Figure 12. The switching turn-on and turn-off timing vs. the salient position

The rise and fall angles are incorporated with the rotor position information. These switching angles are variable and depend on the rotation speed and desired current command in the phase windings of the SRM. To improve the performance of SRM drives, several approaches had been proposed and focused on the inductance measurement related issues [11-14]. Figure 13 illustrated the concept of computing to obtain proper switching timing.
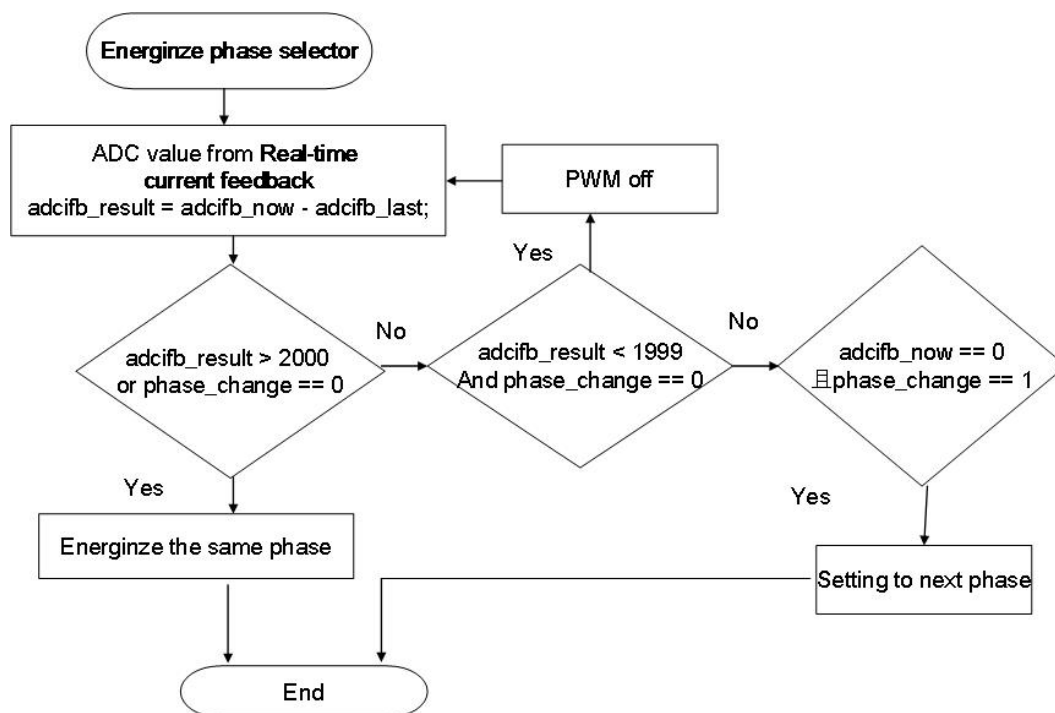
Figure 13. Block diagram of the energize phase selector

The current transducer and proximity sensor feedback base on energized phase current and instantaneous rotor position to compare the current gradient. Once the current gradient reduces under a specific value and the stator and rotor salient are achieving alignment position at the same phase, then the energize phase selector should off the PWM or force to energize next phase. The strength of the proposed method is no to increase the equipment cost and achieve the goal with a simple algorithm to decide the timing of phase change.

4.1.3 Velocity estimation
The rotor position is sensed by proximity sensor which generates a pulse train. The pulse train estimates the speed by a digital algorithm. It counts the plus times in 100 millisecond timeframe. The timeline of

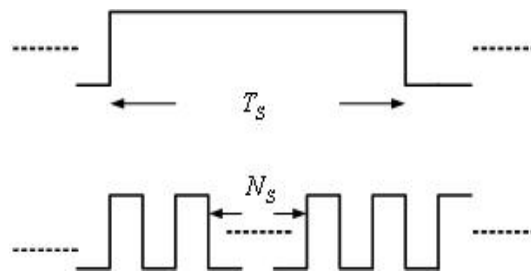velocity estimator algorithm is shown in Figure 14.

Figure 14. The timeline of velocity estimator algorithm

In case of three phases 12/8 pole SRM, it has 48 times pulse train per one revolution. Base on the equation (19), the resolution of proximity sensor is 48 plus per revolve.

$$\omega_r = K_C \times \frac{N_s}{T_s} \tag{19}$$

where: T_s is Sampling time, N_s is The proximity sensor pulse train during sampling time.

However, the algorithm occupies one pulse deviation, in theory, it may exist a ±12.5 rpm tolerance. The expression can be written as:

$$\pm 1(pulse) \times \frac{1}{48}(rev/pulse) \times \frac{1}{0.1}(1/\sec) \times 60 = \pm 12.5 rpm \tag{20}$$

The SRM rotor salient position must be linkup to DSP controller. Once the rotor rotates more than 15 mechanical degrees, the proximity sensors sense the rotor position has changed and input new position into DSP ADC converter for decoding. The information is applied to estimate the velocity as illustrated in the Figure 15. The velocity estimation is executed during the timer ISR notify a new position measurement has been received.
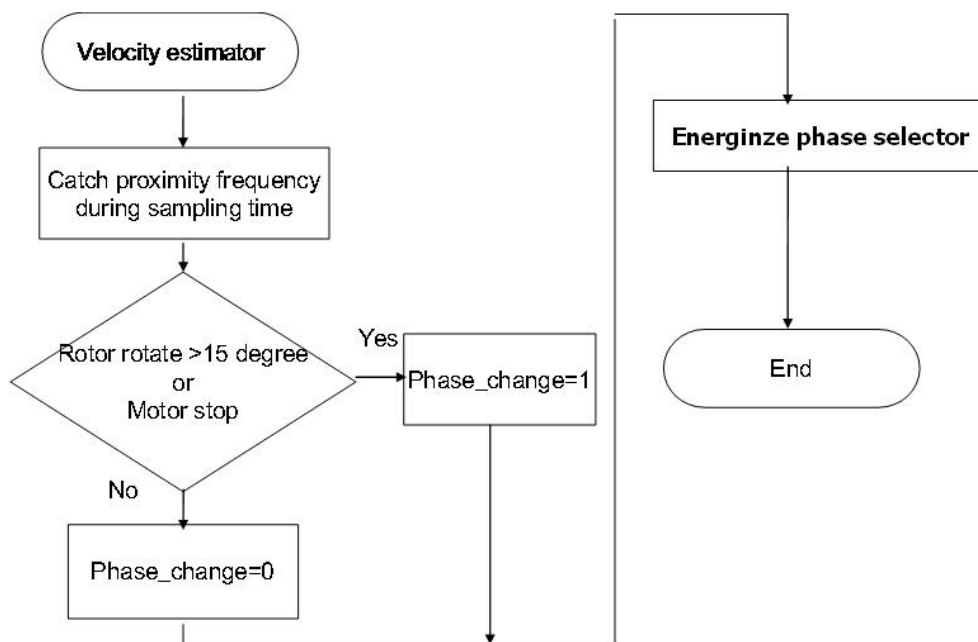

Figure 15. The velocity estimator algorithm

The energize phase selector algorithm is different between the motor starting and running. Figure 16 represents the case when the SRM start, the controller infers a phase has been energized by the proximity sensor status. However, the rotor may be align or opposite rotation direction might achieved, so the DSP should communicate with the velocity estimator to confirm the SRM start as expected.

After the SRM started, the velocity estimator calculates the rotor rotation speed. If the electrical angle is within assigned range, the DSP ADC converter catches the feedback by current transducer to survey the duty cycle for the next energization. The phase selector for running is illustrated in the Figure 17.
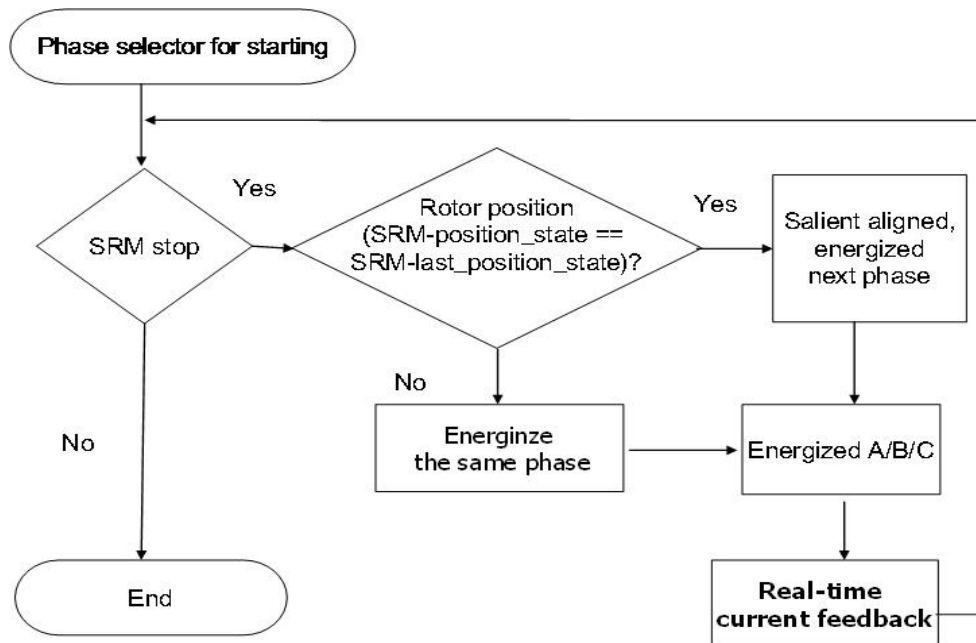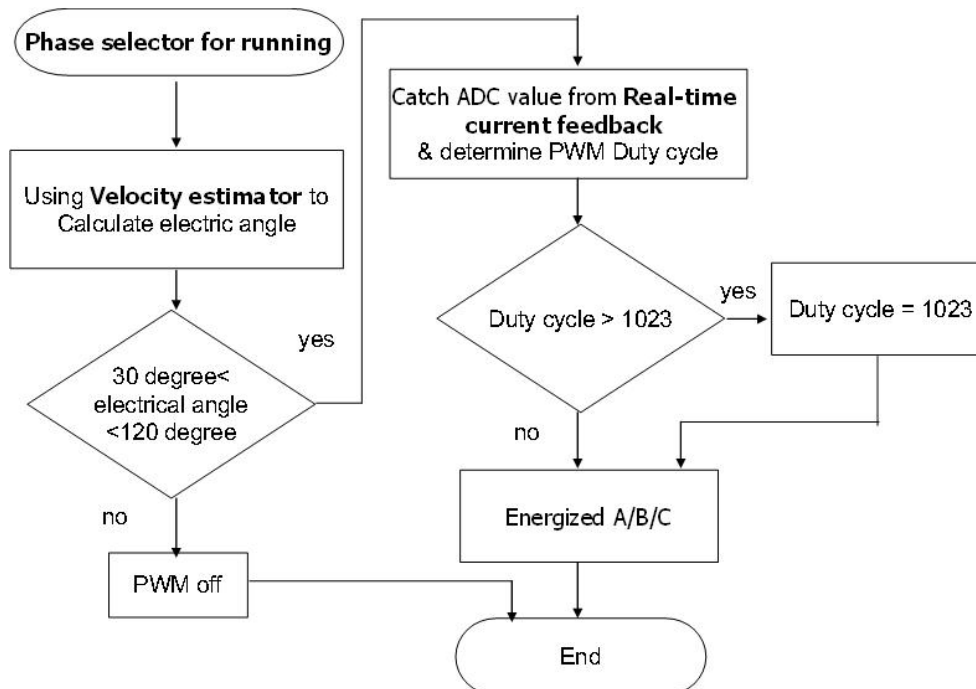

Figure 16. The phase selector for SRM starting

Figure 17. The phase selector for SRM running

4.2 Current controller
The TMS320F240 accomplishes compare units and output logic to regulate fixed-frequency programmable PWM signals with varying duty cycles. The percentage of duty cycle command is calculated by the closed-loop feedback of current transducer. The voltage reference subtracts from PWM carrier to modulate the duty cycle of the output. The result of the current and voltage PWM regulator trend to retain almost the same shape of waveform at a wide speed range.

The current feedback is required. The torque increases when the current is increasing. Once the current is low, the torque is roughly proportional to the current squared. But at high currents, it becomes more nearly linear. At very high currents, the flux saturation decreases the torque per ampere again. The current feedback program flow is proposed in Figure 18.
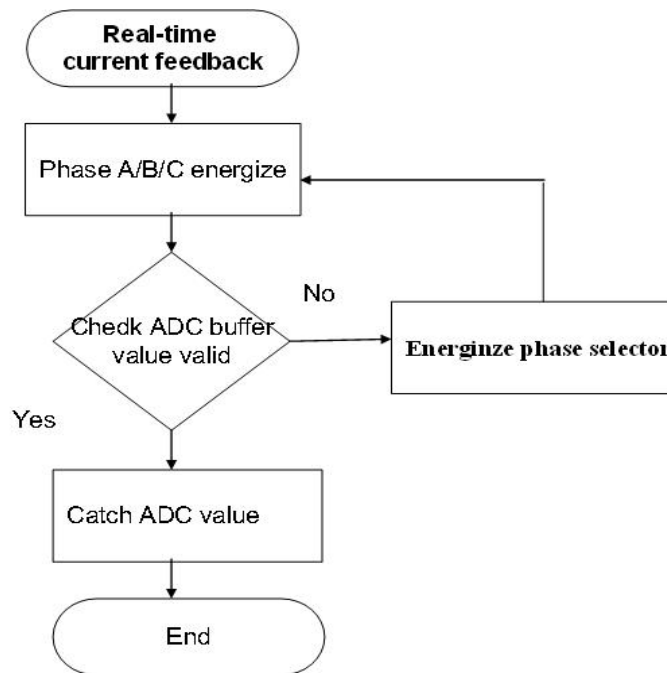

Figure 18. The real-time current feedback flowchart

The torque command is obtained using the torque constant multiplied by the current command, the torque constant is formed from the linearity inductance vs. rotor position characteristics in a particular value of current. Each phase current is individually regulated using a fixed-frequency PWM inverter.

Often, the proportional plus integral (PI) controller is used for a simple control law to achieve a stable performance. The current transducer value is subtracted from the current command to obtain Δi_x, then multiply by the constant of proportion. The result is the proportion error. The accumulation integration error $I\_\Delta i_x$ obtained by the former $I\_\Delta i_x$ plus the proportion error Δi_x. The sum of both values determines the duty ratio of PWM switching current for each windings. The output of the current controller is the current command. It inputs to the PWM to generate the three-phase current to provide a smooth operation of the SRM.

4.3 Velocity controller and high speed protection
The speed command is obtained from the command interface circuit. The velocity controller is activated when receiving the speed error. The design of the velocity controller is a simple PI as the equation (21)

$$u(t) = K_p \cdot e(t) + K_i \cdot \int_0^t e(t)dt \qquad (21)$$

The velocity estimator feedbacks the velocity error by a closed-loop manner to compare the desired velocity command with current velocity. It also accumulates the integral error. The PI controller compensates the velocity error to achieve the steady-state velocity and outputs a signal to the speed error

command. PI controller also limits the torque command of the energize phase selector to prevent over loading.

The velocity controller also provides a smooth and soft operation of the SRM, and the velocity commend can be modify by the VR of commend interface circuit anytime. In order to protect the component to be damaged by switching to opposite rotation at high velocity, the protection function is developed in the control system. To avoid increasing any hardware cost, the implementation is embedded in the velocity controller. Figure 19 shows the algorithm of the high speed protection for opposite operation.

Once the SRM running, the velocity estimator informs the direction and rotation speed to the DSP. If the velocity is less than a specific safety range, the SRM accepts the opposite rotate command and proceeds to rotate. In case the velocity is higher than the safety range, the DSP shuts down the PWM immediately and idles for the error reset [15-17].
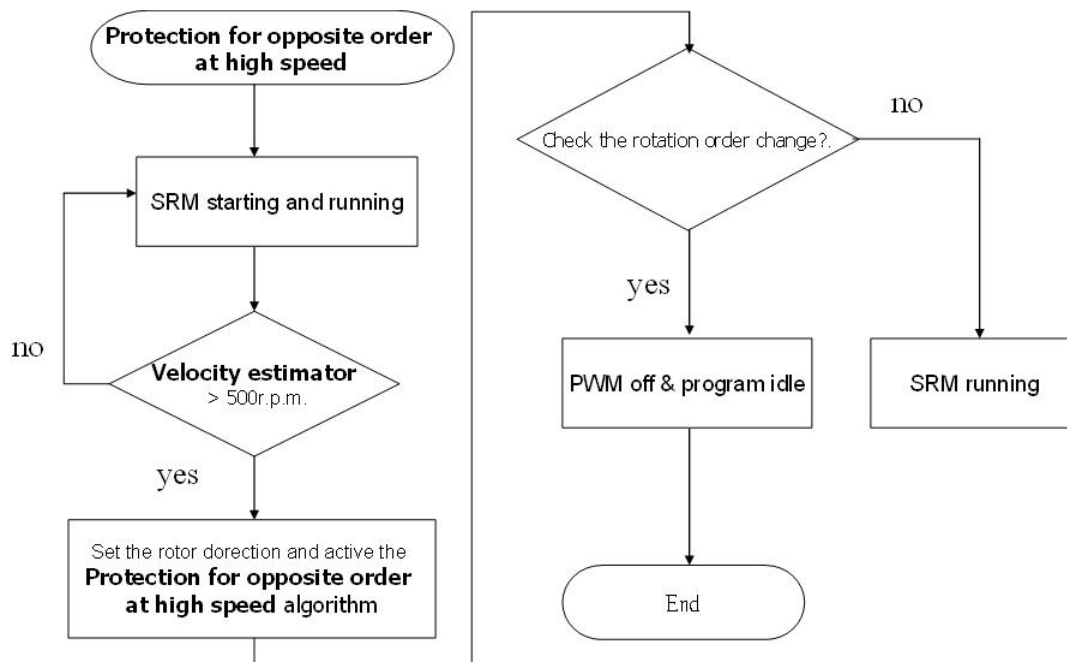

Figure 19. High speed protection for opposite operation

5. Experimental results

The SRM is controlled by high-speed and real-time DSP controller, it is operated with current transducer and proximity sensors. In order to achieve a higher dynamic performance, the system controls the torque current and the speed, dealing with highly nonlinear characteristics.

The velocity is the first characteristic to be surveyed in the overall controller performance. The current waveform is in relation with the performance of the torque; two current diagrams will be shown in the result, one from the oscilloscope and the other from a current transducer. This signal is feed backed to the DSP. The object to be controlled in the experiment is Emerson part number H55PWBKB-1833 three phase 12/8 pole SRM. The specifications are listed in Table 2.

Table 2. Emerson H55PWBKB-1833 three phase 12/8pols SRM specification
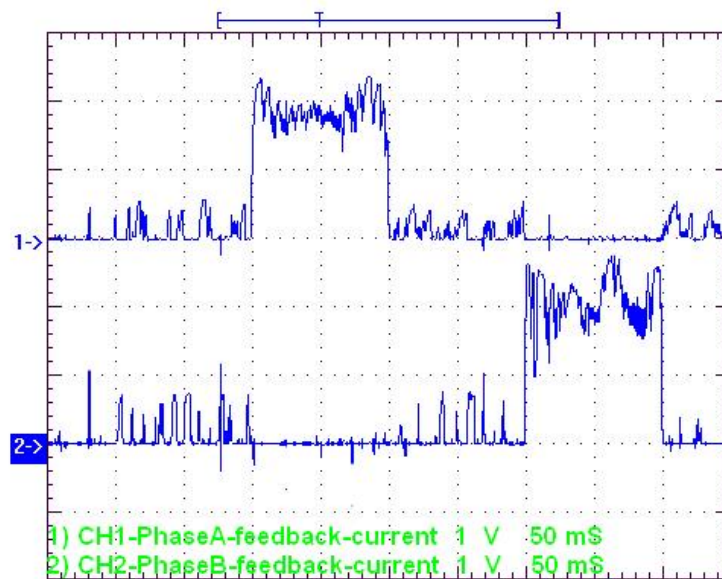
Phase	3
Stator poles	12
Rotor poles	8
Stator winding resistor	2.2Ω
Maximum inductance of the stator winding	28.525mH
Minimum inductance of the stator winding	6.553mH
Rate capacity	120V、2.5A
Rate velocity	1500rpm

5.1 Peak phase current algorithm

The experimental scheme is proposed for hybrid sensor feature with current and velocity control strategy to change the energized phase at the specific salient alignment position by the peak phase current as shown in Figure 20(a) and (b).
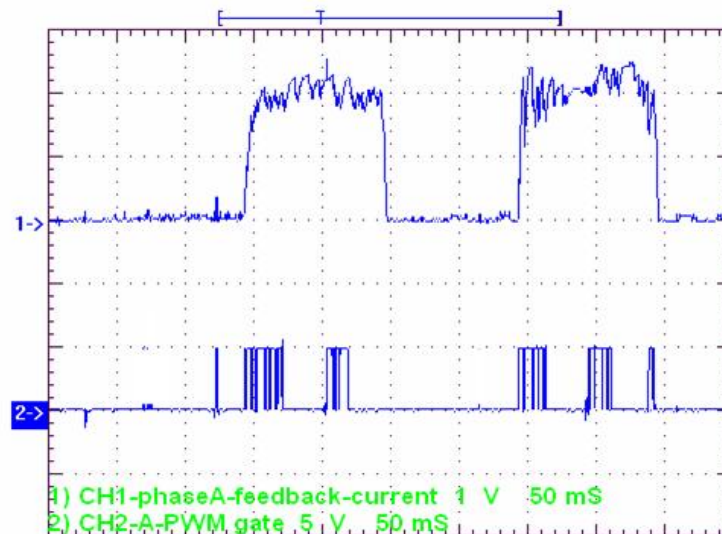

(a)

(b)

Figure 20. The peak phase current algorithm (a) the phase A current transducer and gate driver signal, and (b) the phase A and phase B current transducer

5.2 Variable speed control result

In this part, the system implementation is illustrated to a given velocity command by command interface board at clockwise rotation 1500, 2000 rpm and anti-clockwise denote -1500 and -2000 rpm velocity command and current response.

Figure 21(a) and (b) shows the velocity and current response of 1500 rpm velocity command, Figure 21(c) is the phase A current transducer and gate driver signal. Figure 22(a) and (b) show the velocity and current response of 2000 rpm velocity command, Figure 22(c) is the phase A current transducer and gate driver signal. Figure 23(a) and (b) show the velocity and current response of -1500 rpm velocity command. Figure 24 (a) and (b) show the velocity and current response of -2000 rpm velocity command.
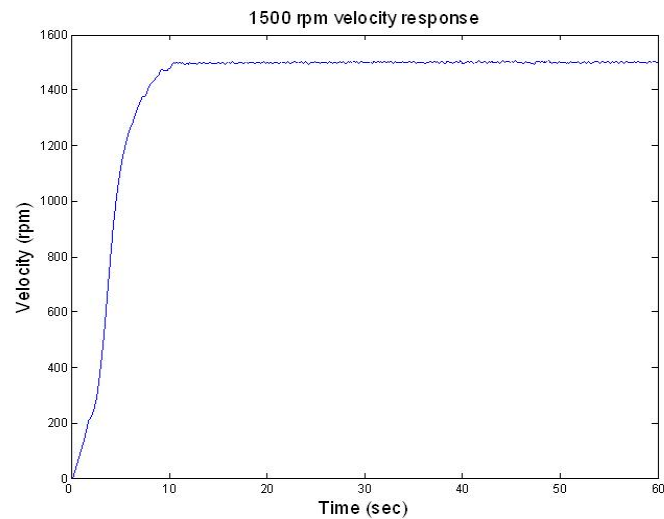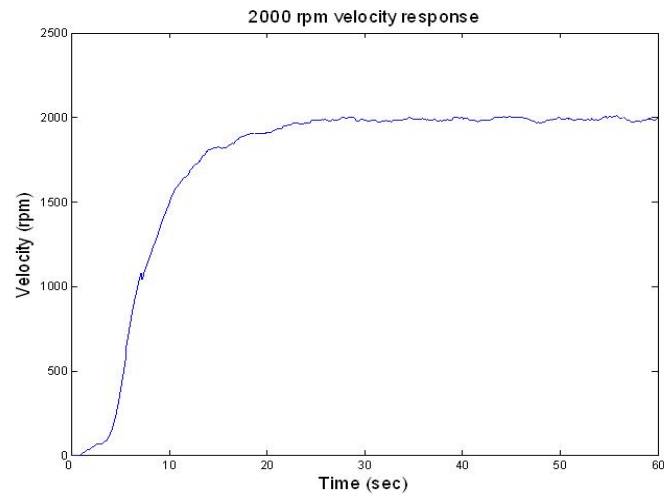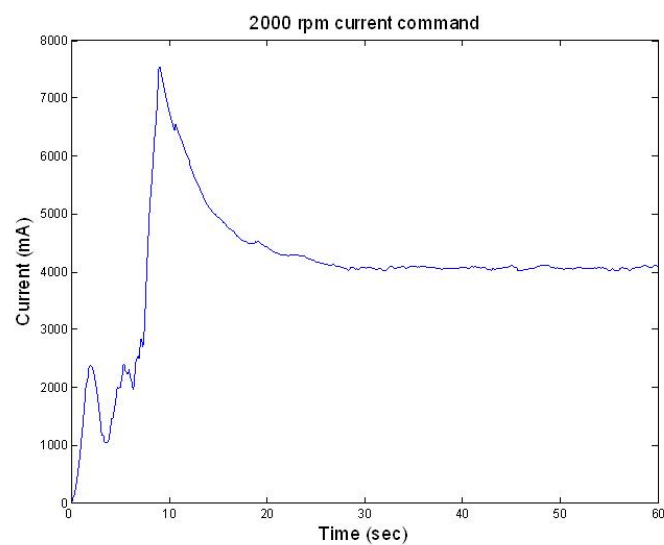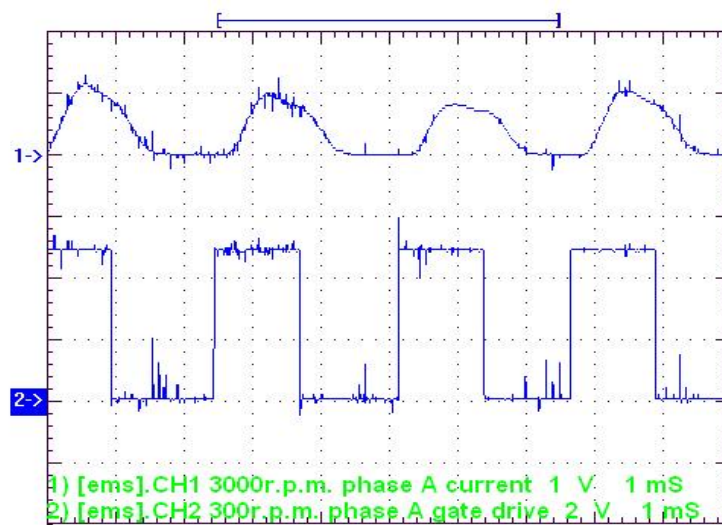
(a)
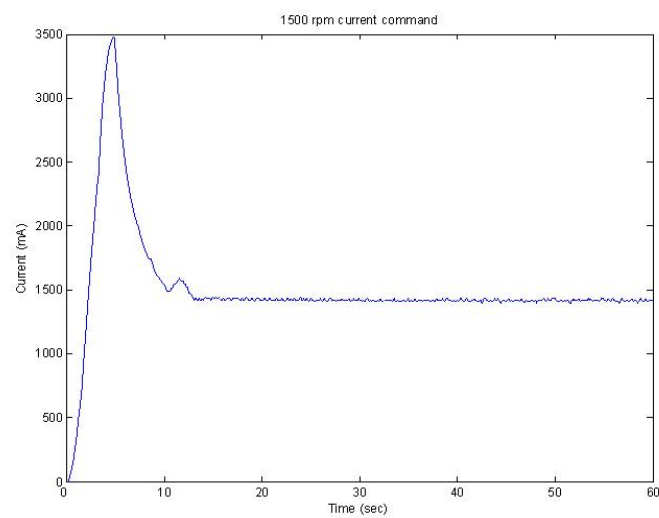
(b)
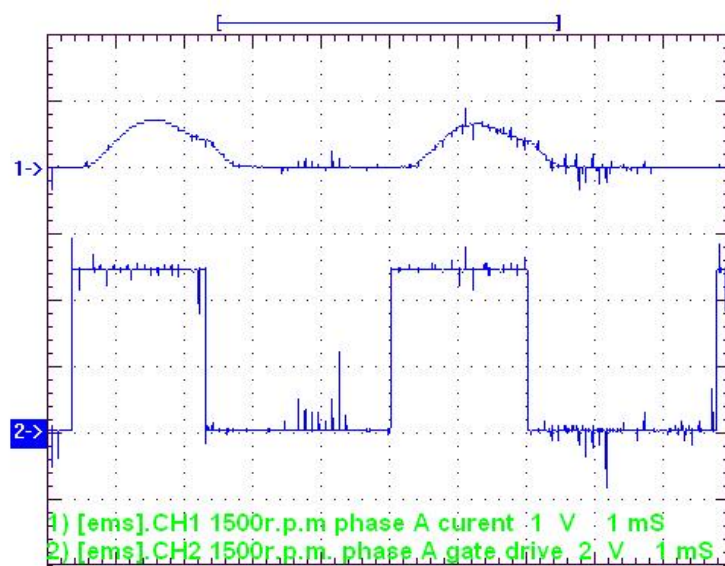
(c)

Figure 21. The velocity command 1500 rpm (a) the velocity response, (b) current response, and (c) phase A current transducer and gate driver signal
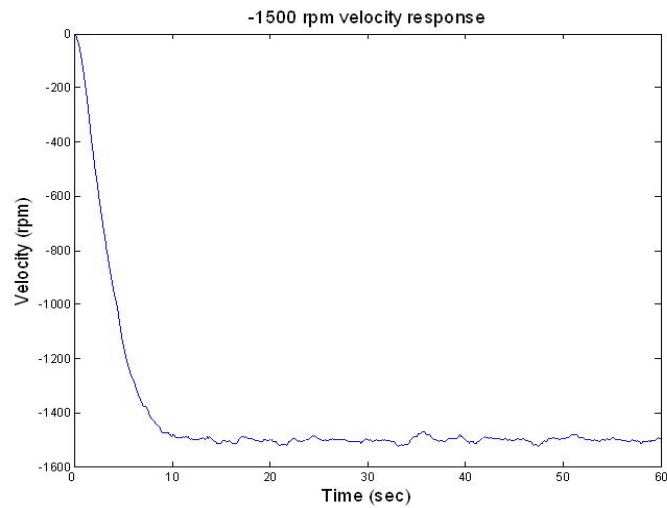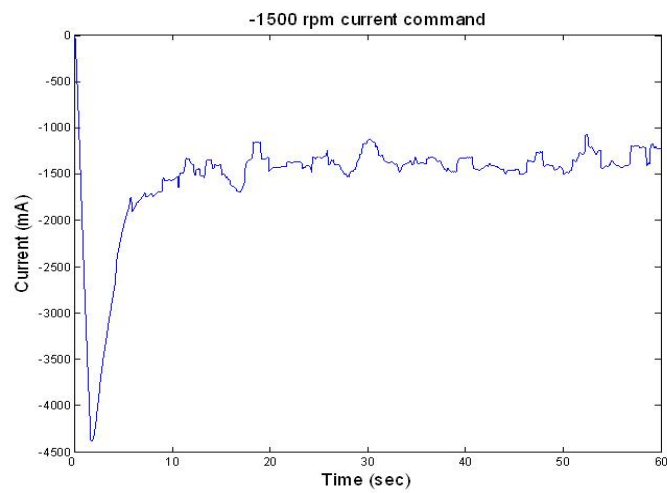
(a)

(b)

(c)

Figure 22. The velocity command 2000 rpm (a) the velocity response, (b) current response, and (c) phase A current transducer and gate driver signal.
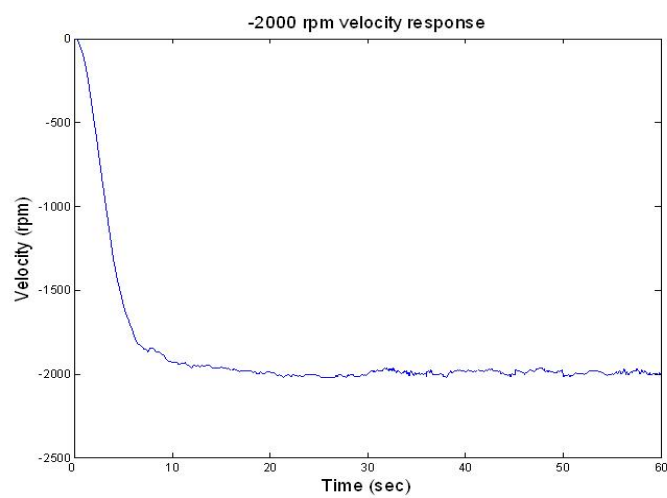
(a)

(b)

Figure 23. The velocity command -1500 rpm (a) the velocity response, and (b) current response

(a)

(b)
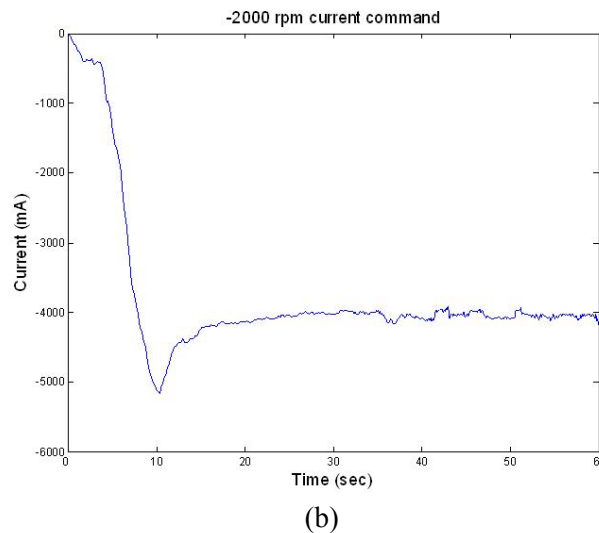
Figure 24. The velocity command -2000 rpm (a) the velocity response, and (b) current response

5.3 Operate protection

The protection function is demonstrated in case of the opposite rotate command at the current velocity is higher than the safety range. Here, the safety range is set at 500 rpm. The velocity and current response are shown in Figure 25(a), (b).

(a)

(b)

Figure 25. The protect function when rotation higher than 500 rpm (a) velocity response, and (b) current response

6. Conclusion

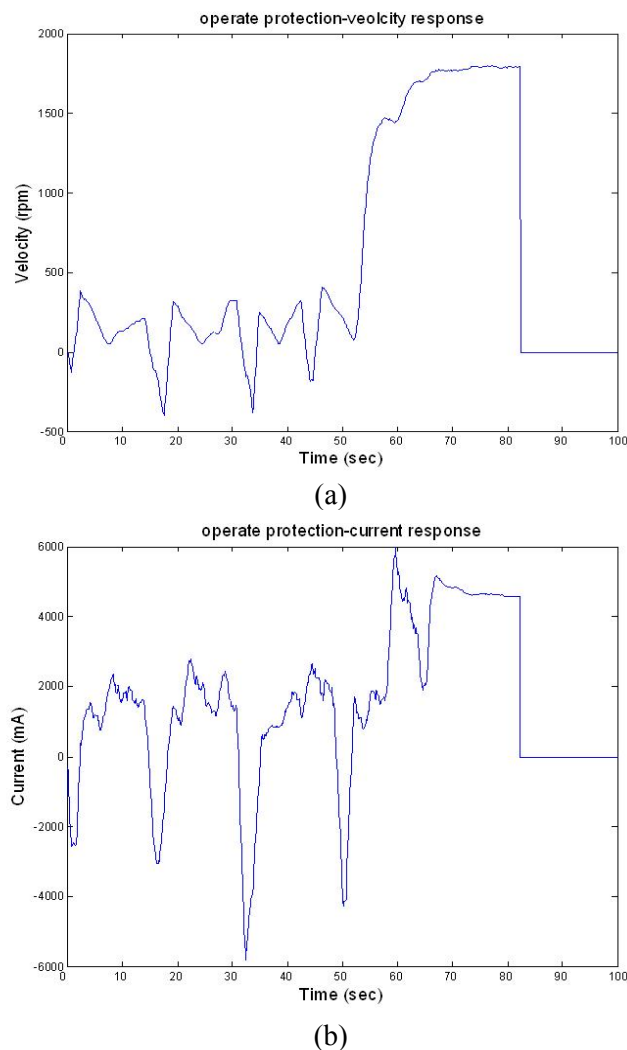The SRM is a robust, reliable and almost maintenance free device for variable speed application. The DSP-based hybrid sensor controller performed as expected with variable speed response and minimum torque ripple, resulting on a reduced speed oscillation which is suitable to be used in industries and transporter applications. The controller produced moderate performance at a wide speed response without complicated calculation.

Both of SRM characteristics set, flux/current/position and torque/current/position, are nonlinear. This is required for SRM drives with motion sensors. In principle, the SRM apparently is less attractive for servo applications. However, the motor simplicity and ruggedness is suitable for variable speed applications.

References

[1]   Miller T. J. E. Switched reluctance motor and their control: Magna Physics Publishing and Clarendon Press Oxford, 1993.

[2]   Miller T. J. E. Brushless Permanent-Magnet and Relutance Motor Drives: Clarendon Press Oxford, 1989.

[3]   Krishnan R. Switched reluctance motor drives : modeling, imulation, analysis, design and applications, C.R.C. Press, 2001.

[4]   Lu W., Keyhani A., Klode H., Proca A.B. Modeling and parameter identification of switched reluctance motors from operating data using neural networks. IEEE IEMDC 03, pp. 1709 -1713, 2003.

[5]   Mese E., Torrey D. A. An approach for sensorless position estimation for switched reluctance motor using artificial neural networks. IEEE Trans. Power Electronics. 2002, 17, 66-75.

[6]   Ehsani M., Husain I., Ramani K.R., Galloway J.H. Dual-decay converter for switched reluctance motor drives in low-voltage application. IEEE Transactions on Power Electronics. 1993, 8, 224-230..

[7]   Becerra R. C., Ehsani M., Miller T. J. E. Commutation of SR motor. IEEE Transactions on Power Electronics. 1993, 8, 257-263.

[8]   Pollock C., Williams B.W. Power Converter Circuits for Switched Reluctance Motors with the Minimum Number of Switches. IEE Proceedings on Electric Power Applications. 1990, 137(6), 373-384.

[9]   Husain I., Ehsani M. Rotor position sensing in switched reluctance motor drives by measuring mutually induced voltage. IEEE Transactions on Industry Applications. 1994, 30(3), 665-672.

[10]   Ehsani M., Ramini K. R. Direct control strategies based on sensing inductance in switched reluctance motors. IEEE Transactions on Power Electronics, 1996, 11(1), 74-82.

[11]   Husain and Ehsani M. Torque ripple minimization in switched reluctance motor drives by PWM current control. IEEE Transactions on Power Electronics, 1996, 11, 85-88.

[12]   Moallem M., Ong C. M., Unnewehr L. E. Effect of rotor profiles on the torque of a switched reluctance motor. IEEE Industry Applications Society Annual Meeting, pp.247-253, 1990.

[13]   Davis R. M. Variable reluctance rotor structures-their influence on torque production. IEEE Transactions on Industrial Electronics. 1992, 39(2), 168-174.

[14]   Pollock C., Williams B.W. A unipolar converter for a switched reluctance motor. IEEE Transactions on Industry Applications. 1990, 26, 222-228.

[15]   Barnes M., Pollock C. Power electronic converters for switched reluctance drives. IEEE Transactions on Power Electronics, 1998, 13(6), 1100-1111.

[16]   Heva A. M., Blasko V., Lipo T. A. A Modified C-Dump Converter for Variable-Reluctance Machines. IEEE Transactions on Industry Applications, 1992, 28(5),1017-1022.

[17]   Panda S. K., Zhu X. M., Dash P. K. Fuzzy gain scheduled PI speed controller for switched reluctance motor drive. IEEE Proceeding of IECON, pp. 989-994, 1997.
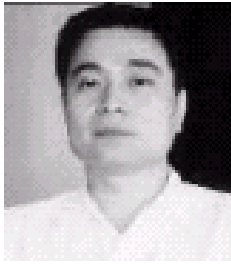
Whei-Min Lin was born on October 3rd, 1954. He received his BS-EE from the National Chao-Tung University, MS-EE from the University of Connecticut, and his PH.D. EE from the University of Texas, Arlington, in 1985. He worked at Chung-Hwa Institute for Economic Research, Taiwan, as a visiting researcher after his graduation. He joined Control Data Crop. in 1986 and worked with Control Data Asia in 1989. He has been with National Sun Yat-Sen university, Taiwan, since 1989. Dr. Lin's interests are GIS, Distribution System, SCADA and Automatic Control System. Dr. Lin is a member of IEEE and Tau Beta Pi.
E-mail address: wmlin@mail.ee.nsysu.edu.tw

Chih-Ming Hong was born on September 17, 1972. He received the MS-EE degree from the Chung Yuan Christian University, Chung Li, Taiwan, R.O.C., in 1999. He is currently pursuing his Ph.D. degree at National Sun Yat-Sen University, Kaohsiung, Taiwan, R.O.C.. His research interests include motor servo drives, control theory applications, and the wind energy conversion systems.
E-mail address: d943010014@student.nsysu.edu.tw

Chiung-Hsing Chen was born in 1961. He received the B.S. degree in electrical engineering from the Feng Chia University, Taichung, Taiwan, in 1983 and M.S. and Ph.D. degree in electrical and computer engineering from the Ohio University, OHIO, USA, in 1994. Currently, he is with National Kaohsiung Marine University, Taiwan, where has been since 1994. His main interests are DSP, SCADA, and intelligent control.
E-mail address: chiung@mail.nkmu.edu.tw

Huang -Chen Chien was born on August 9, 1973. He received the B.S. degree in electrical engineering from the National Kaohsiung University of Applied Science, Kaohsiungi, Taiwan, R.O.C., in 1999 and the M.S. degree in electrical engineering from the National Sun Yan-Sen University, Kaohsiung, Taiwan, in 2008. His research interests include DSP, power motor drive and Semiconductor packaging.
E-mail address: anderson.chien@cande.com.tw